Available online at www.sciencedirect.com

ScienceDirect

Procedia CIRP 111 (2022) 359–362

www.elsevier.com/locate/procedia

12th CIRP Conference on Photonic Technologies [LANE 2022], 4-8 September 2022, Fürth, Germany

Signal processing of airborne acoustic emissions from laser metal deposited structures

Julian Ulrich Weber[a,*], Michael Knabe[a], Vurgun Sayilgan[b], Claus Emmelmann[c]

[a]Fraunhofer Research Institution for Additive Manufacturing Technologies IAPT, Am Schleusengraben 14, 21029 Hamburg, Germany
[b]Laser Zentrum Hannover e.V., Hollerithallee 8, 30419 Hannover, Germany
[c] Institute of Laser and Systems Technology, Hamburg University of Technology, Harburger Schloßstr. 28, 21079 Hamburg, Germany

* Corresponding author. Tel.: +49 40 484010-780; fax: +49 40 484010-999. *E-mail address:* julian.ulrich.weber@iapt.fraunhofer.de

Abstract

Laser Metal Deposition (LMD) is an additive manufacturing process that enables the production of complex structures on existing parts. To reduce the use of costly and energy-intensive produced materials like titanium, these structures can be selectively deposited on favorable but differing substrate materials. However due to differing material characteristics, this results in a high defect potential.
Extensive process parameter development and online process monitoring helps to minimize the impact of defect formation. Monitoring of airborne acoustic process emissions can be used to identify critical defects early during the process and gain information about process stability.
Two approaches for in-process time-frequency monitoring of the acquired acoustic data were compared within this work: The short time Fast Fourier Transformation and the Continuous Wavelet Transformation. Performance criteria based on detected distinct defect events were defined to evaluate both approaches and define specifications for an Acoustic Emission In-Process Monitoring system.

Keywords: Additive Manufacturing; In-Process Monitoring; Acoustic Emissions; CWT; STFT

1. Introduction

Laser Metal Deposition (LMD) is an Additive Manufacturing (AM) process that uses energy from a laser beam and metallic feedstock in the form of powder to either produce metallic coatings on existing part components or to build up near net-shape structures on given substrate materials. The process offers the opportunity to manufacture complex, functional structures with a high material efficiency and high deposition rates on existing part components [1].

Therefore, LMD presents a favorable manufacturing technique for materials that are costly and complex to process, such as shape memory alloys like Nickel-Titanium (NiTi). By adding NiTi structures on part components, smart integrated actuator functions can be integrated to existing parts and triggered by applying temperature changes [2].

Yet, adding LMD structures on existing parts that usually consist of dissimilar substrate materials, challenges arise for the defect-free LMD process. Build-up defects such as interlaminar delamination and surface-near cracks tend to occur due to differing (inter)metallic phases and its mechanical properties. Recent research investigated the defect formation for the deposition of NiTi on Ti substrate material and developed LMD process parameters and corresponding build-up strategies to improve build-up quality [3–5].

Besides extensive development of individual process parameters, LMD process monitoring can be used to improve build-up quality, acquire central information on process signatures or control critical process parameters. Tang et al. reviewed several monitoring techniques that can be used to monitor metal-based LMD processes. Acoustic emission (AE)

10.1016/j.procir.2022.08.039

monitoring can be used to acquire relevant data with respect to defect formations such as cracks, pores and delamination [6].

1.1. Acoustic Emission signal analysis

Recent research shows the application of AE monitoring to identify defects [7–9], monitor powder mass flow rates [10] or control critical LMD process parameters such as the working distance between substrate material and LMD processing head [11]. AE monitoring offers a variety of applications and is comparably simple to integrate, yet further research in several aspects, for instance in data processing of AE monitoring data is required for a broad industrial application [6].

Air-borne AE signals are usually acquired by microphones that include a capacitor coupled to a membrane. The membrane starts to move when being excited by sound waves and causes changes in voltage dependent on amplitude and frequency of the sound waves. For further investigation of the time-resolved AE signal, occurring frequencies often have to be analyzed to identify and filter distinct frequencies. Most approaches use Short Time Fourier Transformation (STFT), a form of Fast Fourier Transformation (FFT), to transform time-resolved data into frequency-resolved data [9, 11].Traditional FFT decomposes a signal into its component sine functions of various frequency, amplitude and phase. During STFT, the signal is separated into equally spaced windows. For their duration, the signal can be estimated to be quasi-stationary. On these windows, the FFT is applied. This yields a time-frequency spectrum and bandpass filter characteristics, that are constrained by the window size. [12, 16].

FFT methods are an efficient approach to investigate time-frequency data due to low computational effort, however FFT methods usually do not work well for short duration (transient) events. This is explained by the time-frequency trade-off, the uncertainty principle of signal analysis, which is referring to Heisenberg's uncertainty principle. It states that an increase in time resolution leads to a decreasing frequency resolution. Thus, a big window size results in a high time-resolution but low-frequency resolution and vice versa [12, 13].

Non-stationary transient events, such as AE excited by defect formation within LMD structures, might not be identified by STFT-based analysis. Time locations of transient events are only identifiable by applying relatively small window sizes [16]. However, to clarify the detectability of all relevant events and its corresponding frequencies, an alternative transformation approach with non-stationary characteristics and time-variant characteristics has to be performed.

1.2. Data processing with Continuous Wavelet Transform

Continuous Wavelet Transform (CWT) uses wavelets instead of sine functions to decompose the signal and gain data regarding frequency and amplitude. Wavelets are functions that rapidly increase, oscillate around a zero mean and rapidly decay. For the signal decompensation, the wavelets are stretched or compressed in the frequency domain, which compares to the characteristics of a bandpass filter. While window type and size constrain the bandpass filter characteristics in STFT, stretching or compressing of the wavelet, the center frequency of the bandpass filter is shifted higher or lower. Wavelets of different scales and shifts are convolved with the original signal to determine occurring frequencies in the original signal. At lower frequencies, the data will be resolved finely in the frequency domain while at higher frequencies, the data will have higher resolution in the time domain [14, 15].

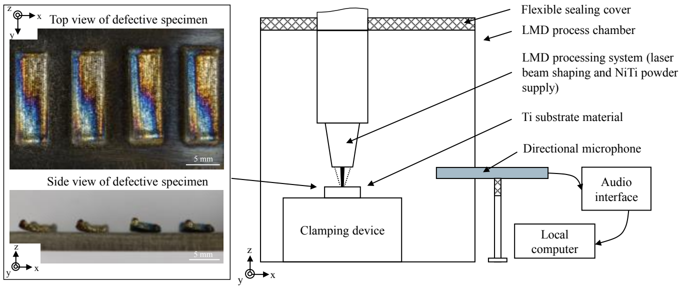

Fig. 1. Welding samples with bonding (l.) defects and schematic drawing of experimental LMD and monitoring setup (r.)

Transient events are characterized as impulsive and are expected to have broad signature in the frequency domain. Therefore, a fine resolution at high frequencies is assumed to be not necessary. Nevertheless, the improved time resolution of the CWT is expected to be beneficial when analyzing transient events and deliver more detailed information of the AE monitoring signals. Within this work, the suitability of STFT for the identification of transient events is investigated by applying CWT to the AE monitoring signal. For this purpose, evaluation criteria are defined to compare and benchmark both approaches with regards to an AE-based In-Process monitoring system for LMD processes.

2. Methods

For the LMD process, a Nd:YAG laser with a wavelength of 1070 nm was used. The processing unit contained an optical system with movable collimation system to reach focal spot diameters between 0.48 mm and 3.52 mm. Argon gas (Ar) was used as shielding and carrier gas (average shielding gas rate of 5 l/min), to achieve a residual O_2 concentration of approx. 200 ppm within the process chamber. The powder mass flow was controlled by a disk-conveying powder feeding system. LMD experiments were carried out using pre-alloyed NiTi powder material (Ni 50.8 at. %, Ti 49.2 at. %). Two LMD experiments (exp. 1 and exp. 2) were performed with an average laser power of 150 W, focal spot diameter of 0,48 mm, welding speed of 11,5 mm/s and a powder feed rate of 2,15 g/min. Rectangular structures with a total of 5 layers were deposited on Ti substrate material. As expected, the material build-up on Ti substrate formed bonding defects between substrate material and deposited material, depicted in Fig. 1.

A directional microphone (*Sennheiser MKE 600*) was used to acquire AE signals. The frequency response of the capacitor microphone ranges from 40 Hz to 20 kHz. The geometrical

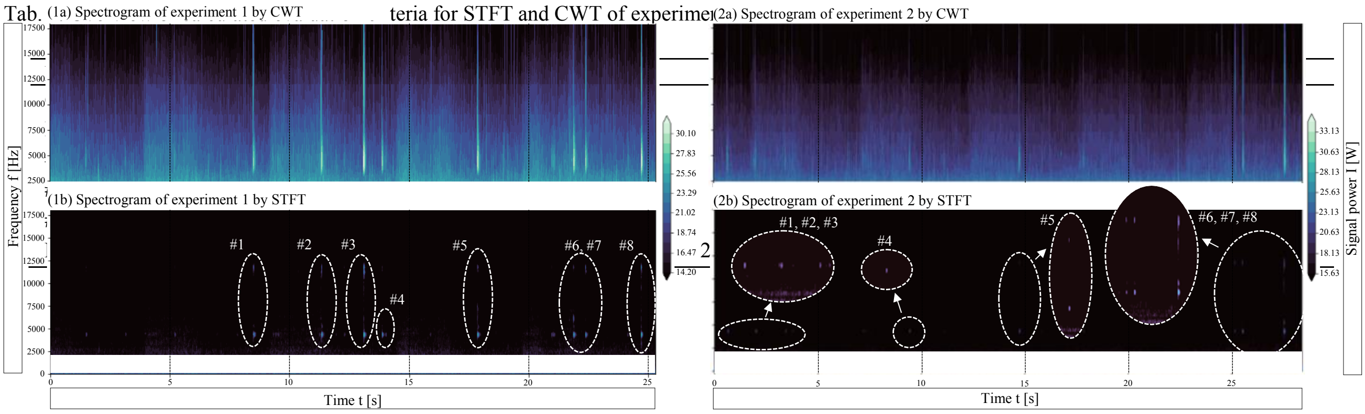

Fig. 2. Spectrograms of both experiments (1 – left, 2 - right) calculated by (a) CWT and (b) STFT.

audio monitoring performance is characterized as super cardioid. The experimental setup is illustrated in Fig. 1.

The sensor output was transformed into a digital signal by an audio interface (*Behringer U-Phoria UMC202HD*) with a maximum sampling rate of 192 kHz. An audio file (.wav, 44100 Hz sampling rate) was generated using *Audacity*.

The acquired audio emission data was processed using *Python* programming language and *MATLAB*-based libraries (*Numpy, pywt, SciPy*). The decomposition by STFT and CWT of audio files results in spectrograms that show frequency (f in Hz) over time data (t in s) with the corresponding signal power level (I in W) for each data point. For a close relation to human perception, the Morlet wavelet was used for CWT. To simplify the decomposition by STFT, a constant window size and type (Hann window) was used. An investigation of different window sizes and types was not focused within this work. The spectrograms were analyzed visually with a focus on the transient events. Additionally, quantifiable evaluation criteria that help to describe the processed data and the transient events were defined.

Transient events are expected to have a much higher intensity compared to ground noise. To count the relevant transient events, intensity thresholds I_{thres} (80 % of max. intensity (I_{max})) are defined. All frequency-time data points above I_{thres} are counted with n_{thres}. Further, main transient events were identified by clustering of n_{thres} in time segments and concluded in the number of main transient events n_{trans}. To evaluate the accuracy in frequency of the main transient events, the frequency range f of the events was identified. The computational effort of both transformation approaches is evaluated by comparing the computational time t_s, which is measured for the calculation of the spectrograms.

3. Results

Fig. 2 shows the spectrogram of the acquired AE monitoring signal corresponding to the welding samples in Fig. 1. For both experiments, all possible frequencies with its corresponding intensities have been calculated using the CWT and STFT. Due to high calculation effort for frequencies below 2500 Hz and above 18000 Hz, the spectrograms range from 2500 to 18000 Hz.

As assumed, all spectrograms developed by CWT show more details compared to the spectrograms calculated by STFT. This is visualized by the higher range of occurring frequencies in the spectrograms. Especially the CWT spectrogram of exp. 2 shows a lot more blue, turquoise and bright green (equals frequency intensities between approximately 21 – 30 W) colors compared to the STFT spectrogram, where frequency intensities are dominantly visualized with black, corresponding to the lower end of frequency intensity with 17 W.

Delamination occurred during the LMD process, that are expected to correlate to transient events. In the spectrograms they are visualized by clearly visible peaks and lines. By focusing on intensities above I_{thres}, 8 peaks can be identified for both experiments. CWT shows, that those critical events occurred after approx. 8 s, 11,2 s, 13 s, 14 s, 17,8 s, 22 s, 22,5 s and 24,7 s. The frequency of the events range between 3000 and 18000 Hz. Comparing the events of CWT to STFT spectrograms, it is visible that short peaks can be identified at the same time markers. Visually, every transient event that is clearly identifiable with CWT-based spectrograms is also identifiable with STFT-based spectrograms. It further stands out, that all visually identifiable peaks within STFT-based spectrograms correlate to high intensity peaks within CWT-based spectrograms. Tab. 1 summarizes the evaluation criteria of both transformation approaches and experiments.

Corresponding to the spectrograms, the evaluation criteria show, that the CWT produces more data points and thus offers a more detailed analysis of AE monitoring signals. Exp. 1 yields n_{total} of 7811846 using CWT compared to 383680 data using STFT, while exp. 2 yields n_{total} 8772050 data points using CWT compared to 430848 data points with STFT. The higher data density results in higher computational time t_s for both experiments: 14 and 19 s are needed with STFT while 163 and 187 s of computational time is needed with CWT for both approaches being implemented in Python programming language. Thus, CWT calculates approx. 20 times more data points compared to STFT in the same computational circumstances. CWT offers a more detailed description of transient events with n_{thres} of 69563 (exp. 1) and 1094 (exp. 2), resulting in approx. 0.890 % (exp. 1) and 0.012 % (exp. 2) transient event data points per n_{total}. STFT yields n_{thres} of 137 (exp. 1) and 64 (exp. 2), resulting in 0.036 % (exp. 1) and 0.015 % (exp. 2) transient event data points per n_{total}. Therefore, the probability to detect transient event data can be described as similar for both approaches. Furthermore, the narrow frequency band for transient events in STFT-based spectrograms is confirmed by the frequency range with frequencies between 4130…11890 Hz compared to the full bandwidth of 2500…17500 Hz for CWT-based data for exp 1. By clustering data points n_{thres} manually to time segments, $n_{cl,trans}$ can be calculated. Both approaches identify 8 transient events visually for both experiments.

CWT delivers more detailed data, due to higher resolution in time compared to STFT. Unlike STFT, CWT is able to produce high time-resolution without decreasing frequency-resolution. The identified frequency range of occurring transient events with CWT data is wider compared to STFT data. The high range of identified frequency spectrum can be explained by the limitations in the frequency-resolution for CWT, that arise due to limitations in computational power and due to dependence of frequency-resolution on occurring height of occurring frequencies.

An AE-based LMD In-Process monitoring system is expected to identify critical events, such as cracks and delamination defects. It is shown, that delamination links to transient events with distinct frequencies within the AE monitoring data. The identification of transient events is challenging for STFT; however, it is shown that all transient events were identified by both approaches. It is concluded that STFT is a suitable transformation approach with less computational effort for an AE-based LMD In-Process monitoring system.

4. Conclusion

This work investigated the suitability of STFT as data processing technique for an AE-based LMD In-Process monitoring system, that requires to identify critical AE events being excited by cracks or delamination defects within the LMD processed structure. LMD structures with delamination defects were produced while AE process emissions were being monitored. By means of comparison to more detailed decomposition of the AE monitoring signal by CWT, it is shown that STFT data delivers less information of the AE monitoring signal with, yet all critical events could be identified with distinct frequencies and less computational effort. The identification of critical events was performed by the analysis of transient events within the AE monitoring data. Conclusively, STFT was evaluated to be suitable for an AE-based LMD In-Process monitoring system. Due to the occurrence of delamination defects only, the transient events are assumed to correlate to delamination.

However further research is required to evaluate criticality of transient events and quantify defects by AE monitoring data. For defect correlation, an in-process imaging of the defect formation is required. Further, image and data processing technologies have to be evaluated for further analysis of transient events and quantification of defects.

References

[1] M. L. B. Möller, Prozessmanagement für das Laser-Pulver-Auftragschweißen. Berlin, Heidelberg: Springer Berlin Heidelberg, 2021.

[2] G. B. KAUFFMAN and I. MAYO, “The Story of Nitinol: The Serendipitous Discovery of the Memory Metal and Its Applications,” Chem. Educator, vol. 2, 1997.

[3] J. U. Weber, A. Bauch, J. Jahnke, and C. Emmelmann, “Acoustic emissions of laser metal deposited NiTi structures,” Proceedings of Lasers in Manufacturing LIM, 2021.

[4] C. Scheitler, O. Hentschel, T. Krebs, K. Y. Nagulin, and M. Schmidt, “Laser metal deposition of NiTi shape memory alloy on Ti sheet metal: Influence of preheating on dissimilar build-up,” Journal of Laser Applications, vol. 29, 2017.

[5] C. A. Biffi, A. Tuissi, and A. G. Demir, “Martensitic transformation, microstructure and functional behavior of thin-walled Nitinol produced by micro laser metal wire deposition,” Journal of Materials Research and Technology, vol. 12, 2021.

[6] Z. Tang et al., “A review on in situ monitoring technology for directed energy deposition of metals,” Int J Adv Manuf Technol, vol. 108, 2020.

[7] L. W. Koester, H. Taheri, L. J. Bond, and E. J. Faierson, “Acoustic monitoring of additive manufacturing for damage and process condition determination,” AIP Conference Proceedings 2102, 2019.

[8] A. La García de Yedra et al., “Online cracking detection by means of optical techniques in laser-cladding process,” Struct Control Health Monit, vol. 26, 2019.

[9] H. Gaja and F. Liou, “Defects monitoring of laser metal deposition using acoustic emission sensor,” Int J Adv Manuf Technol, vol. 90, 2017.

[10] J. Whiting, A. Springer, and F. Sciammarella, “Real-time acoustic emission monitoring of powder mass flow rate for directed energy deposition,” Additive Manufacturing, vol. 23, 2018.

[11] T. Hauser, R. T. Reisch, T. Kamps, A. F. H. Kaplan, and J. Volpp, “Acoustic emissions in directed energy deposition processes,” Int J Adv Manuf Technol, 2022.

[12] J. Allen, “Short term spectral analysis, synthesis, and modification by discrete Fourier transform,” IEEE Trans. Acoust., Speech, Signal Process., vol. 25, 1977.

[13] H. Zeng, Z. Zhou, Y. Chen, H. Luo, and L. Hu, “Wavelet analysis of acoustic emission signals and quality control in laser welding,” Journal of Laser Applications, vol. 13, 2001.

[14] H. Guo and C. S. Burrus, “Convolution using the undecimated discrete wavelet transform,” in 1996 IEEE International Conference on Acoustics, Speech, and Signal Processing Conference Proceedings, Atlanta, GA, USA, 1996.

[15] S. G. Mallat, “A theory for multiresolution signal decomposition: the wavelet representation,” IEEE Trans. Pattern Anal. Mach. Intell., vol. 11, 1989.

[16] I. Y. H. Gu, M. Bollen, “Time-frequency and time-scale domain analysis of voltage disturbances,” IEEE Trans. on Power Delivery 15, 2000.